Measurement of Inclusive Radiative B-Meson Decays with a Photon Energy Threshold of 1.7 GeV

A. Limosani,[20] H. Aihara,[40] K. Arinstein,[1,29] T. Aushev,[17,11] A. M. Bakich,[36] V. Balagura,[11] E. Barberio,[20] A. Bay,[17] K. Belous,[10] M. Bischofberger,[22] A. Bondar,[1,29] A. Bozek,[26] M. Bračko,[19,12] T. E. Browder,[6] P. Chang,[25] Y. Chao,[25] A. Chen,[23] B. G. Cheon,[5] Y. Choi,[35] J. Dalseno,[7] M. Danilov,[11] A. Drutskoy,[2] W. Dungel,[9] S. Eidelman,[1,29] P. Goldenzweig,[2] B. Golob,[18,12] H. Ha,[15] H. Hayashii,[22] Y. Hoshi,[38] W.-S. Hou,[25] H. J. Hyun,[16] K. Inami,[21] R. Itoh,[7] Y. Iwasaki,[7] T. Julius,[20] D. H. Kah,[16] H. O. Kim,[16] S. K. Kim,[34] Y. I. Kim,[16] Y. J. Kim,[4] K. Kinoshita,[2] B. R. Ko,[15] S. Korpar,[19,12] M. Kreps,[14] P. Križan,[18,12] P. Krokovny,[7] T. Kuhr,[14] R. Kumar,[31] Y.-J. Kwon,[44] S.-H. Kyeong,[44] T. Lesiak,[26,3] J. Li,[6] C. Liu,[33] D. Liventsev,[11] R. Louvot,[17] A. Matyja,[26] K. Miyabayashi,[22] H. Miyata,[28] Y. Miyazaki,[21] R. Mizuk,[11] T. Mori,[21] M. Nakao,[7] H. Nakazawa,[23] S. Nishida,[7] K. Nishimura,[6] O. Nitoh,[42] T. Nozaki,[7] S. Ogawa,[37] T. Ohshima,[21] S. Okuno,[13] H. Ozaki,[7] G. Pakhlova,[11] C. W. Park,[35] H. Park,[16] L. E. Piilonen,[43] M. Rozanska,[26] H. Sahoo,[6] Y. Sakai,[7] O. Schneider,[17] J. Schümann,[7] C. Schwanda,[9] A. J. Schwartz,[2] K. Senyo,[21] M. E. Sevior,[20] M. Shapkin,[10] V. Shebalin,[1,29] C. P. Shen,[6] J.-G. Shiu,[25] J. B. Singh,[31] S. Stanič,[45] M. Starič,[12] K. Sumisawa,[7] T. Sumiyoshi,[41] S. Suzuki,[32] G. N. Taylor,[20] Y. Teramoto,[30] K. Trabelsi,[7] T. Tsuboyama,[7] S. Uehara,[7] Y. Unno,[5] S. Uno,[7] P. Urquijo,[20] Y. Ushiroda,[7] G. Varner,[6] K. E. Varvell,[36] K. Vervink,[17] C. H. Wang,[24] M.-Z. Wang,[25] P. Wang,[8] Y. Watanabe,[13] R. Wedd,[20] J. Wicht,[7] E. Won,[15] B. D. Yabsley,[36] H. Yamamoto,[39] Y. Yamashita,[27] Z. P. Zhang,[33] T. Zivko,[12] and A. Zupanc[12]

(Belle Collaboration)

[1]*Budker Institute of Nuclear Physics, Novosibirsk*
[2]*University of Cincinnati, Cincinnati, Ohio 45221*
[3]*T. Kościuszko Cracow University of Technology, Krakow*
[4]*The Graduate University for Advanced Studies, Hayama*
[5]*Hanyang University, Seoul*
[6]*University of Hawaii, Honolulu, Hawaii 96822*
[7]*High Energy Accelerator Research Organization (KEK), Tsukuba*
[8]*Institute of High Energy Physics, Chinese Academy of Sciences, Beijing*
[9]*Institute of High Energy Physics, Vienna*
[10]*Institute of High Energy Physics, Protvino*
[11]*Institute for Theoretical and Experimental Physics, Moscow*
[12]*J. Stefan Institute, Ljubljana*
[13]*Kanagawa University, Yokohama*
[14]*Institut für Experimentelle Kernphysik, Universität Karlsruhe, Karlsruhe*
[15]*Korea University, Seoul*
[16]*Kyungpook National University, Taegu*
[17]*École Polytechnique Fédérale de Lausanne (EPFL), Lausanne*
[18]*Faculty of Mathematics and Physics, University of Ljubljana, Ljubljana*
[19]*University of Maribor, Maribor*
[20]*University of Melbourne, School of Physics, Victoria 3010*
[21]*Nagoya University, Nagoya*
[22]*Nara Women's University, Nara*
[23]*National Central University, Chung-li*
[24]*National United University, Miao Li*
[25]*Department of Physics, National Taiwan University, Taipei*
[26]*H. Niewodniczanski Institute of Nuclear Physics, Krakow*
[27]*Nippon Dental University, Niigata*
[28]*Niigata University, Niigata*
[29]*Novosibirsk State University, Novosibirsk*
[30]*Osaka City University, Osaka*
[31]*Panjab University, Chandigarh*
[32]*Saga University, Saga*
[33]*University of Science and Technology of China, Hefei*
[34]*Seoul National University, Seoul*
[35]*Sungkyunkwan University, Suwon*
[36]*University of Sydney, Sydney, New South Wales*
[37]*Toho University, Funabashi*

[38]Tohoku Gakuin University, Tagajo
[39]Tohoku University, Sendai
[40]Department of Physics, University of Tokyo, Tokyo
[41]Tokyo Metropolitan University, Tokyo
[42]Tokyo University of Agriculture and Technology, Tokyo
[43]IPNAS, Virginia Polytechnic Institute and State University, Blacksburg, Virginia 24061
[44]Yonsei University, Seoul
[45]University of Nova Gorica, Nova Gorica
(Received 8 July 2009; published 7 December 2009)

Using 605 fb^{-1} of data collected at the $\Upsilon(4S)$ resonance we present a measurement of the inclusive radiative B-meson decay channel, $B \to X_s\gamma$. For the lower photon energy thresholds of 1.7, 1.8, 1.9, and 2.0 GeV, as defined in the rest frame of the B meson, we measure the partial branching fraction and the mean and variance of the photon energy spectrum. At the 1.7 GeV threshold we obtain the partial branching fraction $\mathrm{BF}(B \to X_s\gamma) = (3.45 \pm 0.15 \pm 0.40) \times 10^{-4}$, where the errors are statistical and systematic.

DOI: 10.1103/PhysRevLett.103.241801 PACS numbers: 13.20.He, 13.40.Hq, 14.40.Nd

Radiative B-meson decays $B \to X_s\gamma$ may offer a view of phenomena beyond the standard model of particle physics (SM). These decays proceed via a flavor changing neutral current process; yet to be discovered hypothetical particles, e.g., in the minimal supersymmetric standard model [1] or left-right symmetric model [2], may contribute and cause a sizable deviation from the branching fraction (BF) predicted by the SM. The BF prediction $(3.15 \pm 0.23) \times 10^{-4}$ [3], and the average experimental value $(3.56 \pm 0.26) \times 10^{-4}$ [4], are in marginal agreement. A measurement with improved precision provides a more stringent test and gives stronger constraints on models beyond the SM.

The photon energy spectrum is a direct probe of the b quark's mass and Fermi motion and therefore provides information needed to extrapolate the photon spectrum below the lower photon energy threshold [5], as well as that for the extraction of the SM parameters $|V_{cb}|$ and $|V_{ub}|$ from inclusive semileptonic B decays [6]. The lower the threshold the smaller are their model uncertainties [7].

Belle has previously measured $B \to X_s\gamma$ with 5.8 and 140 fb^{-1} of data using semi-inclusive [8] and fully inclusive approaches [9], respectively. Here we present a new measurement, based on a larger data set and with significant improvements. We cover more of the spectrum by extending the photon energy range from 1.8 down to 1.7 GeV, as measured in the B-meson rest frame. CLEO [10] and *BABAR* [11] reported measurements at lower thresholds of 2.0 and 1.9 GeV, respectively.

We use data collected by the Belle detector at the KEKB asymmetric-energy e^+e^- storage ring [12]. The data consists of a sample of 605 fb^{-1} taken on the $\Upsilon(4S)$ resonance corresponding to 657×10^6 $B\bar{B}$ pairs. Another 68 fb^{-1} sample has been taken at an energy 60 MeV below the resonance (off resonance). The Belle detector is a large-solid-angle magnetic spectrometer described in detail elsewhere [13]. The main component relevant for this analysis is the electromagnetic calorimeter (ECL) made of 16.2 radiation lengths long CsI(Tl) crystals. The photon energy resolution is about 2% for the energy range explored in this analysis.

We extract the signal $B \to X_s\gamma$ spectrum by collecting all high-energy photons, vetoing those originating from π^0 and η decays to two photons. The contribution from non-$B\bar{B}$ processes, referred to as continuum background, mainly $e^+e^- \to q\bar{q}$ ($q = u, d, s, c$) events, is subtracted using the off-resonance sample. The remaining backgrounds from $B\bar{B}$ events are subtracted using Monte Carlo (MC) simulated distributions normalized using data control samples.

Photon candidates are selected from ECL clusters of 5×5 crystals in the barrel region $\cos\theta_\gamma \in [-0.35, 0.70]$, where θ_γ is the polar angle with respect to the beam axis, subtended from the direction opposite the positron beam. They are required to have energies $E_\gamma^{\mathrm{c.m.s.}}$ larger than 1.4 GeV, as measured in the center-of-mass system of the $\Upsilon(4S)$(c.m.s.). Further selection criteria, the same as those applied in Ref. [9], are applied to ensure that clusters are isolated in the ECL and cannot be matched to tracks reconstructed in the drift chamber.

Owing to increased instantaneous luminosity delivered by KEKB, there is a non-negligible background due to the overlap of hadronic events with energy deposits left in the calorimeter by earlier QED interactions (mainly Bhabha scattering). Such composite events are completely separated from the signal using timing information for calorimeter clusters associated with the candidate photons. The cluster timing information is stored in the raw data, and is available in the reduced format used for analysis of data processed after the summer of 2004. Our data set is divided into 254 and 351 fb^{-1} samples that correspond to subsamples without and with cluster timing information, respectively. In the second data set photons that are off time are rejected with a signal inefficiency of 0.2%. In addition, for both sets, we veto any event that contains an ECL cluster with energy exceeding 1 GeV within a cone of 0.2 radians

in the direction opposite our photon candidate in the c.m.s. We employ the same criteria as those used in Ref. [9] to veto candidate photons from π^0 and η decays to two photons.

The analysis proceeds in two different streams, with a lepton tag (LT) and without (MAIN), resulting in final samples that give similar sensitivity to the signal while being largely statistically independent. The lepton tag is employed to suppress continuum background, since the presence of a high momentum lepton is more likely to originate from a primary semileptonic decay of the second B meson in signal events. For an event to be accepted in the LT stream, it must contain a well-identified electron or muon, with momentum between 1.26 and 2.20 GeV/c, at an angle θ_ℓ to the candidate photon such that $\cos\theta_\ell \in [-0.67, +0.87]$, where all measurements are in the c.m.s. The event selection criteria employed to reduce the contribution from continuum events in the MAIN stream are the same as applied in our previous analysis, namely, two Fisher discriminants, relying on energy flow and event-shape variables. Only the second of these discriminants is used in the LT stream with the corresponding coefficients calculated for the lepton tag.

To optimize these selection criteria, we use MC simulated [14] large samples of $B\bar{B}$, $q\bar{q}$, and signal. The signal MC events are generated as a mixture of exclusive $B \to K^*\gamma$ and inclusive $B \to X_s\gamma$ components using EVTGEN [15]. The inclusive component X_s is first generated as a $s\bar{u}$ or $s\bar{d}$ state with spin-1, and then hadronized by JETSET [16]. The relative weights of the two components are chosen to match the world average branching fractions for $B \to K^*\gamma$ and $B \to X_s\gamma$ [4]. To improve the understanding of the photon energy spectrum at low energies, the selection criteria are optimized in the energy bin 1.8 GeV $< E_\gamma^{\text{c.m.s.}} <$ 1.9 GeV.

After these selection criteria we observe 41.1×10^5 (24.6×10^4) and 3.5×10^5 (0.9×10^4) photon candidates in the MAIN (LT) stream of the on- and off-resonance data samples, respectively. The spectrum measured in off-resonance data is scaled by the ratio of the on- to off-resonance luminosity and subtracted. We apply corrections to the yield and energy of candidates derived from the off-resonance sample to account for the effects of the 60 MeV (0.5%) energy difference: a lower cross section and, on average, lower multiplicity and energy of photon candidates.

Beam background is estimated using a sample of randomly triggered events that is added to the $B\bar{B}$ MC. The remnant beam background left after subtraction of non-$B\bar{B}$ background is reduced to a negligible level after the application of the off-time veto. In the sample of data where the veto is unavailable, we scale the background according to a comparison of yields between MC and data for high-energy ($E_\gamma^{\text{c.m.s.}} > 2.8$ GeV) photon candidates found in the end caps of the ECL. This sample after off-resonance subtraction is a clean sample of ECL clusters from beam backgrounds. The ratio of beam background data to MC is found to be 1.16 ± 0.04 in this sample.

From the on-resonance spectrum after continuum background subtraction we subtract backgrounds from B decays. We divide the background into six categories, with relative contributions after selection in the 1.7 GeV $< E_\gamma^{\text{c.m.s.}} <$ 2.8 GeV range as follows for the two streams (MAIN; LT): (i) photons from $\pi^0 \to \gamma\gamma$ (47.4%; 48.0%), (ii) photons from $\eta \to \gamma\gamma$ (16.3%; 16.0%), (iii) other real photons, mainly from decays of ω, η', and J/ψ mesons, and bremsstrahlung, including the short distance radiative correction [17] (8.1%; 8.9%), (iv) ECL clusters not due to single photons, mainly from K_L^0's and $\bar{n}$'s (1.7%; 1.6%), (v) electrons misidentified as photons (6.1%; 3.3%), and (vi) beam background (1.3%; 2.6%). The signal fractions are 19.1% and 19.6%, respectively.

For all of the selection criteria and for each background category we determine the $E_\gamma^{\text{c.m.s.}}$-dependent selection efficiency in off-resonance subtracted data and MC using appropriate control samples as described in Ref. [9]. The ratios of data and MC efficiencies versus $E_\gamma^{\text{c.m.s.}}$ are fitted using low-order polynomials, which are used to scale the background MC. Most are found to be statistically compatible with unity. An exception is the effect of the selection requirements on ECL clusters produced by hadrons: specifically, the requirement that 95% of the energy be deposited in the central nine cells of the 5×5 cluster, which is poorly modeled in the MC simulation. The correction doubles the yield of the hadron background [9].

Each background yield, after having been properly scaled by the described procedures, is subtracted from the data spectrum. The spectra for the MAIN and LT streams are shown in Figs. 1(a) and 1(b), respectively. The photon energy ranges 1.4–1.7 GeV and 2.8–4.0 GeV were chosen *a priori* as control regions to test the integrity of the background subtraction since in the low energy region the little signal expected is negligible with respect to the uncertainty on the background, and no signal is possible in the high-energy region above the kinematic limit. The yields in the high-energy region are 1245 ± 4349 and 292 ± 410 candidates in the MAIN and LT streams, respectively, while corresponding yields in the low energy region are -1629 ± 3071 and -745 ± 623, respectively.

To obtain the true spectrum we correct the raw spectrum in the energy range 1.4–2.8 GeV using a three-step procedure: (i) divide by the probability of a photon candidate satisfying selection criteria given a cluster has been selected in the ECL; (ii) perform an unfolding procedure based on the singular value decomposition (SVD) algorithm [18], which maps the spectrum from measured energy to true energy thereby undoing the distortion caused by the ECL; and (iii) divide by the probability that a photon originating at the interaction point is detected in the ECL.

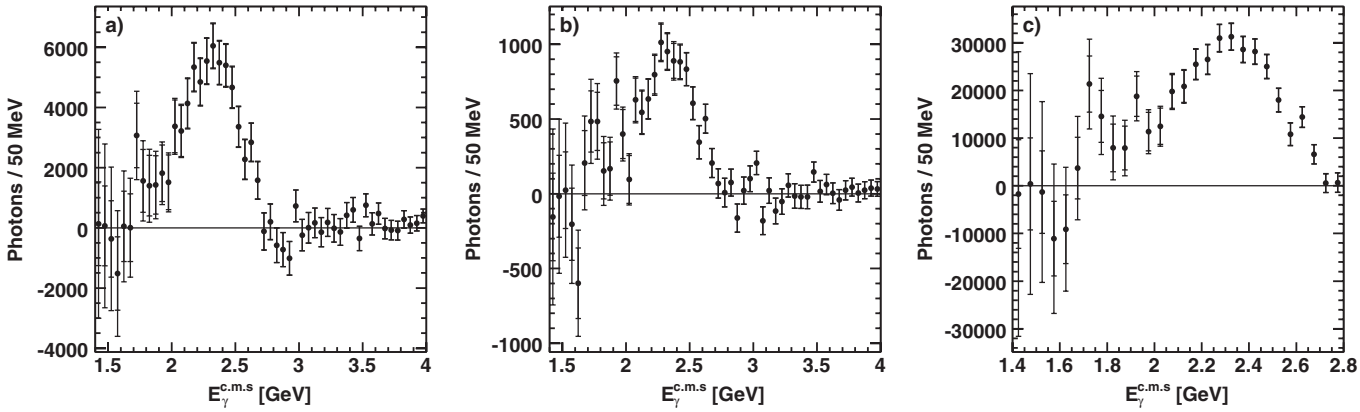

FIG. 1. The extracted photon energy spectrum of $B \to X_{s,d}\gamma$ in the (a) MAIN and (b) LT stream before any correction for signal acceptance is applied; and (c) displays their average after correction by the selection efficiency. The two error bars for each point show the statistical and the total error. The total error is a sum in quadrature of the statistical and systematic errors, where the latter are correlated between bins. The LT and MAIN streams refer to the set of selection criteria that do and do not include the lepton tag criterion, respectively.

The average efficiency of step (i) over the entire range is 15% (2.5%) in the MAIN (LT) stream. The average efficiency of step (iii) is about 80%. Step (ii) eliminates the need to perform corrections for the effect of the ECL resolution on the moments, as was done in Ref. [19], and thereby significantly reduces the large uncertainty due to model dependence. The unfolding matrix, derived from the signal MC sample, is calibrated to data using the results of a study of a clean photon sample from radiative μ-pair events.

A weighted average taking into account the correlation of the MAIN and LT stream spectra is performed after step (i). At this stage the averaging procedure is substantially simplified since there is no statistical correlation between yields in different energy bins. As an example of the cross correlation between the MAIN and LT streams, in the energy bin 2.00–2.05 GeV, there are 116 517 (9834) and 6769 (246) photon candidates in the on-(off-)resonance sample, in the MAIN and LT streams, respectively, of which, 3815 (72) are common to both streams. We find the covariance between the MAIN and LT signal yields is dominated by the overlap of candidates from the off-resonance sample, which is small relative to the individual variances of the MAIN and LT signal yields. This results in a statistical error on the average just above that which is obtained if no statistical correlation is assumed. The spectrum derived from the average of MAIN and LT stream spectra before unfolding is shown in Fig. 1(c).

Our analysis procedure does not distinguish between $B \to X_s\gamma$ and $B \to X_d\gamma$. We subtract the contribution of the latter from all partial branching fraction measurements by assuming the ratio of the branching fractions to be $R_{d/s} = (4.5 \pm 0.3)\%$ [20,21], and thereby assume the shape of the corresponding photon energy spectra to be equivalent. Employing other models for the $B \to X_d\gamma$ photon energy spectrum has a negligible impact on the measured branching fractions and moments of $B \to X_s\gamma$.

To derive the measurements in the rest frame of the B meson we calculate boost corrections using a MC simulation. The corrections are calculated from differences between the spectra in the B-meson and c.m.s. frames. The simulation takes into account the energy of the B meson and its angular distribution in the c.m.s.

Systematic uncertainties are calculated from a number of sources, as given by the numbered list in Table I. We vary the number of $B\bar{B}$ pairs, the on-resonance to off-resonance ratio of integrated luminosities, and the correction factors applied to the off-resonance photon candidates and assign the observed variation as the systematic error associated with continuum subtraction (1). The parameters of the correction functions applied to the MC to calibrate for the effect of selection criteria (2) and those applied to the π^0 and η yields (3) are varied taking into account their correlations. As we do not measure the yields of photons from sources other than π^0's and η's in $B\bar{B}$ events, we independently vary the expected yields of these additional sources by $\pm 20\%$ (4). We vary the corrections applied to beam background data according to their uncertainties (5). For the uncertainties related to the unfolding procedure, we vary the value of the regularization parameter of the SVD algorithm (6). We compare the results from five signal models [22] with corresponding model parameters derived from fits to the signal spectrum derived from the MAIN stream shown in Fig. 1(a). We assign the maximum deviation from the Kagan-Neubert model as the uncertainty (7). The errors associated to the measurement of the photon energy resolution and photon detection efficiency in radiative μ-pair events are varied (8,9), where the former has an uncertainty of 1%. To account for the higher multiplicity hadronic environment of $B\bar{B}$ decays and secondary effects

TABLE I. The measurements of the branching fraction, mean, and variance of the photon energy spectrum for various lower energy thresholds measured in the B-meson rest frame and the contributions to the systematic uncertainty.

	BF($B \to X_s\gamma$) (10^{-4})				$\langle E_\gamma \rangle$ (GeV)				$\Delta E_\gamma^2 \equiv \langle E_\gamma^2 \rangle - \langle E_\gamma \rangle^2$ (GeV^2)			
$E^B_{\gamma\text{-Low}}$ (GeV)	1.70	1.80	1.90	2.00	1.70	1.80	1.90	2.00	1.70	1.80	1.90	2.00
Value	3.45	3.36	3.21	3.02	2.282	2.294	2.311	2.334	0.0428	0.0370	0.0302	0.0230
$\pm$statistical	0.15	0.13	0.11	0.10	0.015	0.011	0.009	0.007	0.0047	0.0029	0.0019	0.0014
$\pm$systematic	0.40	0.25	0.16	0.11	0.051	0.028	0.015	0.009	0.0202	0.0081	0.0030	0.0016
Systematic uncertainties												
1. Continuum	0.26	0.16	0.10	0.07	0.033	0.018	0.009	0.004	0.0111	0.0048	0.0016	0.0005
2. Selection	0.15	0.12	0.10	0.08	0.016	0.009	0.005	0.002	0.0089	0.0029	0.0011	0.0004
3. π^0/η	0.07	0.05	0.04	0.02	0.011	0.006	0.003	0.002	0.0068	0.0022	0.0007	0.0003
4. Other B	0.25	0.14	0.06	0.02	0.033	0.017	0.007	0.002	0.0121	0.0051	0.0017	0.0004
5. Beam bkgd.	0.03	0.02	0.02	0.01	0.002	0.001	0.000	0.000	0.0006	0.0003	0.0001	0.0001
6. Unfolding	0.01	0.01	0.02	0.02	0.006	0.005	0.005	0.004	0.0008	0.0006	0.0005	0.0004
7. Model	0.01	0.01	0.00	0.01	0.002	0.001	0.000	0.001	0.0010	0.0006	0.0004	0.0004
8. Resolution	0.05	0.03	0.01	0.00	0.007	0.004	0.001	0.000	0.0026	0.0011	0.0004	0.0001
9. γ Detection	0.03	0.02	0.00	0.00	0.005	0.003	0.002	0.001	0.0015	0.0007	0.0002	0.0000
10. $B \to X_d\gamma$	0.01	0.01	0.01	0.01	0.000	0.000	0.000	0.000	0.0000	0.0000	0.0000	0.0000
11. Boost	0.01	0.01	0.02	0.02	0.002	0.002	0.004	0.005	0.0012	0.0005	0.0008	0.0009

in the estimation of photons from $B\bar{B}$, we assign twice ($\pm 2\sigma$) the variation as the associated systematic error (9). We find the signal yield as derived after acceptance correction is susceptible to the statistical fluctuations evident in the lower energy region of the photon energy spectrum measured in the LT stream, which propagate from the off-resonance sample.

In the photon energy range from 1.7 to 2.8 GeV, as measured in the B-meson rest frame, we obtain the partial branching fraction: $\mathrm{BF}(B \to X_s\gamma) = (3.45 \pm 0.15 \pm 0.40) \times 10^{-4}$ where the errors are statistical and systematic, respectively. The partial branching fraction, mean, and variance of the photon energy spectrum and the systematic error budget for various lower energy thresholds are given in Table I [23].

In conclusion, for the first time, more than 97% of the $B \to X_s\gamma$ phase space is measured [5] allowing the theoretical uncertainties to be significantly reduced. The measured branching fractions are in agreement with the latest theoretical calculations [3] and are the most precise to date. Our results place tighter constraints on models of new physics [24], where, for example, in the two-Higgs-boson-doublet model II [25], the charge Higgs boson mass is constrained to be above 260 GeV/c^2 at the 95% confidence level [3]. The moment measurements reduce the uncertainty on $|V_{ub}|$. Our measurement supersedes our previous result and will be the last of its type from Belle.

We thank the KEKB group for excellent operation of the accelerator, the KEK cryogenics group for efficient solenoid operations, and the KEK computer group and the NII for valuable computing and SINET3 network support. We acknowledge support from MEXT, JSPS, and Nagoya's TLPRC (Japan); ARC, DIISR, and A. J. Slocum (Australia); NSFC (China); DST (India); MOEHRD and KOSEF (Korea); MNiSW (Poland); MES and RFAAE (Russia); ARRS (Slovenia); SNSF (Switzerland); NSC and MOE (Taiwan); and DOE (USA).

[1] S. Bertolini, F. Borzumati, A. Masiero, and G. Ridolfi, Nucl. Phys. **B353**, 591 (1991).
[2] P. L. Cho and M. Misiak, Phys. Rev. D **49**, 5894 (1994); K. Fujikawa and A. Yamada, Phys. Rev. D **49**, 5890 (1994).
[3] M. Misiak *et al.*, Phys. Rev. Lett. **98**, 022002 (2007); see also T. Becher and M. Neubert, Phys. Rev. Lett. **98**, 022003 (2007).
[4] C. Amsler *et al.* (Particle Data Group), Phys. Lett. B **667**, 1 (2008).
[5] O. L. Buchmüller and H. U. Flacher, Phys. Rev. D **73**, 073008 (2006).
[6] E. Barberio *et al.*, arXiv:0704.3575.
[7] I. Bigi and N. Uraltsev, Int. J. Mod. Phys. A **17**, 4709 (2002); M. Neubert, Phys. Rev. D **72**, 074025 (2005); C. W. Bauer, Phys. Rev. D **57**, 5611 (1998); **60**, 099907 (E) (1999).
[8] K. Abe *et al.*, Phys. Lett. B **511**, 151 (2001).
[9] P. Koppenburg *et al.*, Phys. Rev. Lett. **93**, 061803 (2004).
[10] S. Chen *et al.*, Phys. Rev. Lett. **87**, 251807 (2001).
[11] B. Aubert *et al.*, Phys. Rev. D **72**, 052004 (2005); B. Aubert *et al.*, Phys. Rev. Lett. **97**, 171803 (2006); B. Aubert *et al.*, Phys. Rev. D **77**, 051103 (2008).
[12] S. Kurokawa, Nucl. Instrum. Methods Phys. Res., Sect. A **499**, 1 (2003).
[13] A. Abashian *et al.*, Nucl. Instrum. Methods Phys. Res., Sect. A **479**, 117 (2002).
[14] R. Brun *et al.*, CERN Report No. DD/EE/84-1 (1984).
[15] D. J. Lange, Nucl. Instrum. Methods Phys. Res., Sect. A **462**, 152 (2001).
[16] T. Sjostran *et al.*, Comput. Phys. Commun. **135**, 238 (2001).

[17] E. Barberio and Z. Wąs, Comput. Phys. Commun. **79**, 291 (1994).
[18] A. Höcker and V. Kartvelishvili, Nucl. Instrum. Methods Phys. Res., Sect. A **372**, 469 (1996).
[19] C. Schwanda *et al.*, Phys. Rev. D **78**, 032016 (2008).
[20] T. Hurth, E. Lunghi, and W. Porod, Nucl. Phys. **B704**, 56 (2005).
[21] J. Charles *et al.*, Eur. Phys. J. C **41**, 1 (2005).
[22] A. L. Kagan and M. Neubert, Eur. Phys. J. C **7**, 5 (1999); B. O. Lange, M. Neubert, and G. Paz, J. High Energy Phys. 10 (2005) 084; J. R. Andersen and E. Gardi, J. High Energy Phys. 01 (**2007**) 029; D. Benson, I. I. Bigi, and N. Uraltsev, Nucl. Phys. **B710**, 371 (2005); P. Gambino and P. Giordano (private communication).
[23] See EPAPS Document No. E-PRLTAO-103-158952 for the error correlation matrix. For more information on EPAPS, see http://www.aip.org/pubservs/epaps.html.
[24] For example, O. Buchmüller *et al.*, Phys. Lett. B **657**, 87 (2007).
[25] L. F. Abbott, P. Sikivie, and M. B. Wise, Phys. Rev. D **21**, 1393 (1980).